A Diffusion-Based Two-Dimensional Empirical Mode Decomposition (EMD) Algorithm for Image Analysis

Heming Wang[1], Richard Mann[2], and Edward R. Vrscay[1(✉)]

[1] Department of Applied Mathematics, Faculty of Mathematics, University of Waterloo, Waterloo, ON N2L 3G1, Canada
{h422wang,ervrscay}@uwaterloo.ca

[2] Department of Computer Science, Faculty of Mathematics, University of Waterloo, Waterloo, ON N2L 3G1, Canada
mannr@uwaterloo.ca

Abstract. We propose a novel diffusion-based, empirical mode decomposition (EMD) algorithm for image analysis. Although EMD has been a powerful tool in signal processing, its algorithmic nature has made it difficult to analyze theoretically. For example, many EMD procedures rely on the location of local maxima and minima of a signal followed by interpolation to find upper and lower envelope curves which are then used to extract a "mean curve" of a signal. These operations are not only sensitive to noise and error but they also present difficulties for a mathematical analysis of EMD. Two-dimensional extensions of the EMD algorithm also suffer from these difficulties. Our PDEs-based approach replaces the above procedures by simply using the diffusion equation to construct the mean curve (surface) of a signal (image). This procedure also simplifies the mathematical analysis. Numerical experiments for synthetic and real images are presented. Simulation results demonstrate that our algorithm can outperform the standard two-dimensional EMD algorithms as well as requiring much less computation time.

Keywords: Empirical Mode Decomposition
Partial differential equations · Image analysis · Texture analysis
Local time-frequency analysis

1 Introduction

Empirical Mode Decomposition (EMD), introduced in [12], is a powerful tool for analyzing linear, nonlinear and nonstationary signals. Its ability to perform local time-frequency analysis for nonstationary signals has been demonstrated for real-world signals – see, for example, [1,12,13]. EMD employs a *sifting process* to extract different modes of oscillation of a signal, referred to as *Intrinsic Mode Functions* (IMF). The Hilbert transform is then applied to each IMF in order to determine its instantaneous local frequencies. A repeated application

A. Campilho et al. (Eds.): ICIAR 2018, LNCS 10882, pp. 295–305, 2018.
https://doi.org/10.1007/978-3-319-93000-8_34

of EMD produces a decomposition of a signal into components with decreasing (instantaneous) frequency. The amplitudes and instantaneous frequencies can then produce a local time-frequency analysis of the signal.

Because most of the work on EMD has focused on algorithms as opposed to theoretical analysis, there has been very little work on developing a rigorous theoretical basis for EMD as well as an understanding of why it fails for certain kinds of signals. Many EMD methods rely on rather sensitive, if not questionable, procedures of extracting upper and lower envelopes of a signal from which a mean curve is computed. The mean curve is then used to extract an IMF. In [19], we proposed a novel forward heat equation method to extract the mean envelope which is then used in the sifting process. Our approach is not only more stable but also provides a better mathematical analysis of EMD as well as identifying potential limitations.

There have been a number of efforts to extend EMD to two dimensions [2,4,6,14,16,18,20,21] – these schemes are known as bidimensional EMD (BEMD). Once again, however, these methods lack a sufficient theoretical background due to their algorithmic nature. As in the one-dimensional case, one of the major obstacles of the BEMD method is the extraction of upper and lower envelopes from which *mean surfaces* are computed. Indeed, the extraction procedures performed by many current BEMD algorithms are necessarily much more complicated.

In this paper, we propose a novel, two-dimensional PDE-based BEMD algorithm. The mean surface of a two-dimensional function, e.g., an image, is again obtained by evolving the function according to the diffusion equation, and then employed in a sifting process. Our algorithm has a solid mathematical basis and demonstrates greater effectiveness when applied to images. Moreover, its computational time is lower than that of classical BEMD methods.

2 Classical EMD and BEMD Algorithms

For a given signal $S(x)$, the classical one-dimensional EMD method may be summarized as follows:

1. Find all local maximal points and minimal points of $S(x)$.
2. Interpolate between maximal points to obtain an upper envelope function $E_{upper}(x)$ and between minimal points to obtain a lower envelope function $E_{lower}(x)$.
3. Compute the local mean function: $m(x) = \frac{1}{2}\left[E_{upper}(x) + E_{lower}(x)\right]$.
4. Define $c(x) = S(x) - m(x)$.
5. If $c(x)$ is not an IMF (see note below), iterate $m(x)$ until it is.
6. After finding the IMF, subtract it and repeat Step 2 to obtain the residual.

Note: Most EMD procedures employ the following rather a vague definition of an intrinsic mode function (IMF): (i) The number of extrema and zero-crossings of an IMF must differ at most by one and (ii) the mean of the IMF should be close to zero.

The result of the above procedure is the following decomposition of the signal $S(x)$,

$$S(x) = \sum_{k=1}^{N} c_k(x) + r(x), \tag{1}$$

where $c_k(x)$ is the kth IMF, and $r(x)$ is the residual. Two-dimensional EMD algorithms, i.e., BEMD, follow a similar procedure although the extraction of upper and lower envelopes is understandably much more complex.

As we discuss in [19], the classic EMD algorithm suffers from the following shortcomings: (i) lack of mathematical proof, (ii) errors near borders, (iii) a vague definition of the IMF and (iv) sampling effects. BEMD algorithms such as those in [2,18,21] are based on the classical 1D EMD algorithm which means, unfortunately, that they suffer from similar shortcomings.

One of the major problems of EMD has been the lack of a theoretical framework. There has been a number of efforts to provide a mathematical explanation and basis for EMD. Daubechies *et al.* [5] proposed an EMD-like tool which they called a *synchrosqueezed wavelet transform*. Their algorithm employs wavelet analysis along with a reallocation method and provides a precise mathematical expression for a series of separable harmonic components in the signal.

El Hadji *et al.* [7,8] introduced a backward heat equation approach to interpret the EMD algorithm. For a prescribed $\delta > 0$, they first defined the upper and lower envelopes of a function $h(x)$ as follows,

$$U_\delta = \sup_{|y|<\delta} h(x+y),\ L_\delta = \inf_{|y|<\delta} h(x+y), \tag{2}$$

Because of space limitations, we mention only very briefly the procedures which are then adopted. First, the Taylor expansions of the envelopes are computed from which the following mean envelope function is defined,

$$m_\delta(x) = \frac{1}{2}[U_\delta(x) + L_\delta(x)] \approx h(x) + \frac{\delta^2}{2} h''(x). \tag{3}$$

The sifting process to obtain the IMF is then defined as follows,

$$h_{n+1}(x) = h_n(x) - m_\delta(x)\,, \quad h_0(x) = h(x). \tag{4}$$

Using the following Taylor expansion in t,

$$h_{n+1} = h(x, t + \Delta t) = h_n + \Delta t \frac{\partial h}{\partial t} + O(\Delta t^2) \tag{5}$$

the authors arrive at the following PDE,

$$\frac{\partial h}{\partial t} + \frac{1}{\delta^2} h + \frac{1}{2} \frac{\partial^2 h}{\partial x^2} = 0, \quad h(x, 0) = S(x). \tag{6}$$

Note that this PDE is a *backward* heat equation.

Niang *et al.* [15] proposed the following fourth-order non-linear equation as the interpolator to simulate the spline interpolation of upper and lower envelope,

$$\frac{\partial s(x,t)}{\partial t} = \frac{\partial}{\partial x}\left[g(x,t)\frac{\partial^3 s(x,t)}{\partial x^3}\right], \tag{7}$$

where $g(x,t)$ is the nonlinear diffusivity function. By controlling the non-linear terms, the envelopes will pass through maximal and minimal points.

3 Proposed Diffusion-Based EMD and BEMD Algorithms

As discussed briefly in Sect. 2, most EMD algorithms obtain the mean function from upper and lower envelopes which, in turn, are obtained by interpolating local maxima and minima of a function $S(x)$. All of these procedures are time-consuming and sensitive to error and noise. Our diffusion-based EMD method, on the other hand, is based on the intuition that the mean curve $m(x)$ passes through all inflection points of $S(x)$. The idea is very simple: Instead of taking the average of two envelope functions of a signal $S(x)$ to produce a mean – Step 3 of the classical EMD algorithm in Sect. 2 – we proceed as follows. For a prescribed $\tau > 0$, we define $h_n(x) = h(x, n\tau)$ for $n = 0, 1, 2, \cdots$ and use Eqs. (3) and (4) to obtain the following equation,

$$h_{n+1} = h_n + C\,\frac{\partial^2 h}{\partial x^2}. \tag{8}$$

Note that from this equation, the value of h at its spatial inflection points remains the same. Now apply the following Taylor expansion to h_{n+1},

$$h_{n+1}(x) = h(x, n\tau + \tau) = h(x, n\tau) + \tau\frac{\partial h}{\partial t}(x, n\tau) + o(\tau^2). \tag{9}$$

After a few steps we arrive at the equation,

$$\tau\frac{\partial h}{\partial t} + O(\tau^2) = C\,\frac{\partial^2 h}{\partial x^2}. \tag{10}$$

We now assume that $C = a\tau$ and, after division by τ, arrive at the following initial value problem (IVP) for the heat/diffusion equation,

$$\frac{\partial h}{\partial t} = a\frac{\partial^2 h}{\partial x^2}, \qquad h(x,0) = S(x). \tag{11}$$

For prescribed values of the diffusivity constant $a > 0$ and time $T > 0$ (which can be adjusted) we now define the *mean function* of $S(x)$ as $m(x) = h(x,T)$, i.e., the solution of the IVP in Eq. (11) at time T. In other words, the mean function $m(x)$ is obtained from $S(x)$ by low-pass filtering.

Our method clearly differs from other EMD algorithms since it bypasses (i) the complicated procedure of extracting local maxima and minima of a signal as

well as (ii) the interpolations of these points to obtain upper and lower envelopes. Instead, the mean curve $m(x)$ is obtained directly from the signal by means of smoothing. Unlike the backward heat equation in Eq. (6), the PDE employed in our EMD procedure is a *forward* heat equation. As is well known, forward diffusion is numerically more stable than backward diffusion. Niang's fourth-order PDE in Eq. (7) could be viewed as quite similar to our second-order PDE. However, as a fourth-order diffusion PDE, it will generate significantly more error when dealing with noise in image signals. As such, our second-order PDE should capture the local features of images more effectively.

We extend the above PDE-based EMD method to the two-dimensional case by simply adding another spatial variable to the PDE in (11), i.e.,

$$\frac{\partial h}{\partial t} = D(\frac{\partial^2 h}{\partial x^2} + \frac{\partial^2 h}{\partial y^2}), \qquad h(x, y, 0) = S(x, y, 0). \tag{12}$$

The *mean function* of $S(x, y)$ will be defined as $m(x, y) = h(x, y, T)$.

As in the 1D case, one of the primary motivations for this definition is that the time rate of change of $h(x, y, t)$ is zero at spatial inflection points of h. This is the basis of the following PDE-based BEMD algorithm applied to an image function $S(x, y)$:

1. Initialize: Let $n = 0$ and set $h_0(x, y, 0) = S(x, y)$.
2. Find the mean of $h_n(x, y, 0)$: Solve the PDE in (12) for $h_n(x, y, t)$ for $0 \leq t \leq T$. Then define $m_n(x, y) = h_n(x, y, T)$.
3. Extract mean: Define $c_n(x, y) = h_n(x, y, 0) - h_n(x, y, T)$.
4. If $c_n(x, y)$ is not a BIMF, let $h_{n+1}(x, y, 0) = c_n(x, y)$, $n \to n + 1$ and go to Step 2.

4 Mathematical Interpretation

As mentioned in Fladrin's paper [9], traditional EMD operates as an successive filter. In fact, we claim that traditional EMD operates as an iterative, frequency-overlapping, contrast-sensitive filter bank. This is also the case with our modified EMD and BEMD methods. In each iteration, the mean of the signal is obtained by passing it through a low-pass filter. Subsequent subtraction of the mean from the signal implies that the net procedure is equivalent to a high-pass filter. To illustrate, we consider the following special two-dimensional case,

$$S(x, y) = \sum_{i,j} [A_{ij} \sin(\omega_i x + \omega_j y + \phi_{ij})], \tag{13}$$

where each (i, j) pair represents a single sinusoidal grating basis function. Equation (12) is solved for the first mean function,

$$m_a(x, T) = \sum_{i,j} \frac{1}{\Omega_{ij}^2} [A_{ij} \sin(\omega_i x + \omega_j y + \phi_j)], \qquad \Omega_{ij} = \sqrt{\omega_i^2 + \omega_j^2}. \tag{14}$$

The magnitudes Ω_{ij} are now sorted in increasing order and denoted as Ω_k. We denote the sum of all components with the same Ω_k-value as s_k. After N iterations, our modified EMD algorithm yields the following result for $s_k(x)$,

$$h_{k,N} = (1 - e^{-a\Omega_k^2 T})h_{k,N-1} = (1 - e^{-a\Omega_k^2 T})^N s_k. \tag{15}$$

Now suppose, without loss of generality, that $\Omega_1 < \Omega_2 < \cdots < \Omega_K = \Omega_{\max}$. It is easy to show that for N sufficiently large,

$$h_N = \sum_{k=1}^{N} (1 - e^{-a\Omega_k^2 T})^N s_k \simeq (1 - e^{-a\Omega_K^2 T})^N s_K \simeq s_K, \tag{16}$$

where the final approximation is valid for T sufficiently large. By choosing the appropriate set of parameters, the IMF extracted after N iterations will be (at least approximately) the highest-frequency component, s_K. Our EMD algorithm, however, does not distinguish the direction of a frequency component (i.e., a particular sine grating) because the diffusion is *radial*. Instead, it will filter a group of frequency components Ω_{ij} that have the same "angular magnitude" Ω_k.

5 Experimental Results

We now show some results obtained by applying our diffusion-based EMD algorithm to some synthetic images [3], and some real images [11], A comparison of execution times between our method and classical BEMD is also presented.

Our current algorithm employs the simple explicit finite difference scheme for solving PDEs. There are two options for boundary conditions (BCs): For an image whose edges are part of the background and of the same amplitude level, we have used Dirichlet BCs. For an image with irregularly-shaped boundaries, we have used Neumann BCs.

Simple Sine Grating Image: In Fig. 1, we display results for a 512×512-pixel synthetic image which consists of a mixture of two sine gratings. It has the form,

$$S(x, y) = \sin(0.1\pi x + 0.1\pi y) + \sin(-0.4\pi x + 0.8\pi y), \tag{17}$$

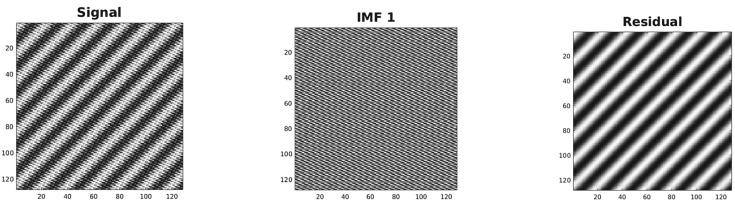

Fig. 1. Simple sine grating separation. **Left:** Sine gratings mixture. **Middle:** First BIMF. **Right:** Residual.

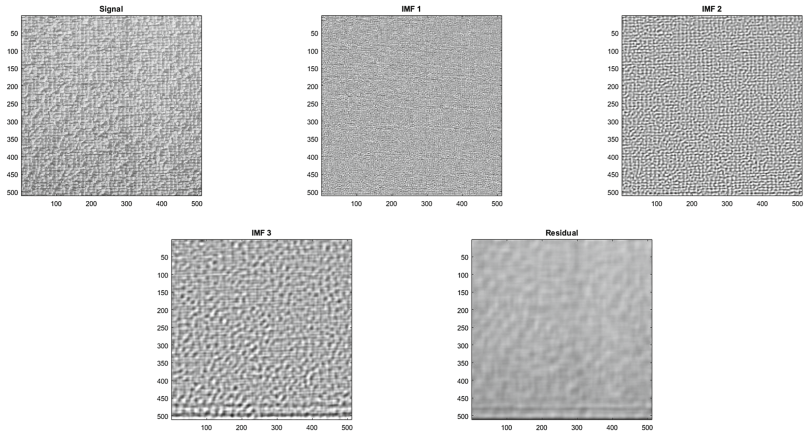

Fig. 2. Example for texture decomposition. **Top row:** Raffia texture image from Brodatz [3], first BIMF and second BIMF. **Bottom row:** Third BIMF and the residual.

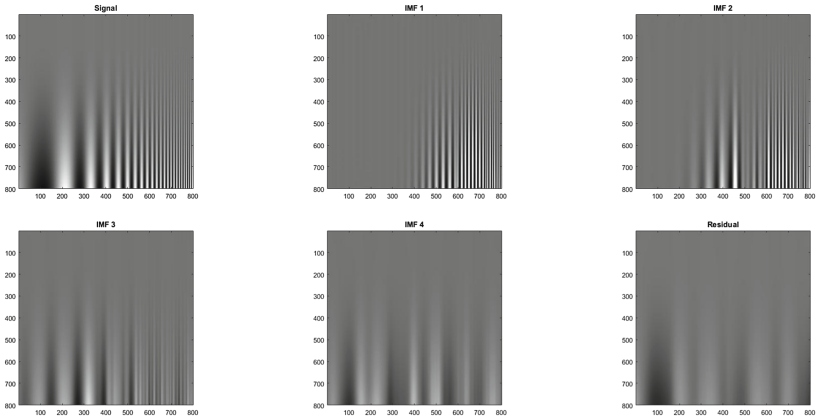

Fig. 3. Contrast sensitive function (CSF) and corresponding BIMFs. **Top row:** CSF, first and second BIMF. **Bottom row:** Third and fourth BIMFs and residual.

The second (higher frequency) component is extracted as the first BIMF and the first component comprises the residual. The two sine gratings have been separated.

Texture Image: In Fig. 2 are shown the BIMF and residual when our diffusion-based BEMD algorithm is applied to a 512×512-pixel texture image selected from [3]. Successive BIMFs are comprised of lower frequency components of the texture.

Contrast-Sensitive Image: The *contrast sensitivity function* (CSF) is an image which demonstrates the sensitivity of an observer to sine wave gratings of differing spatial frequencies [17]. Different frequency components are amplified

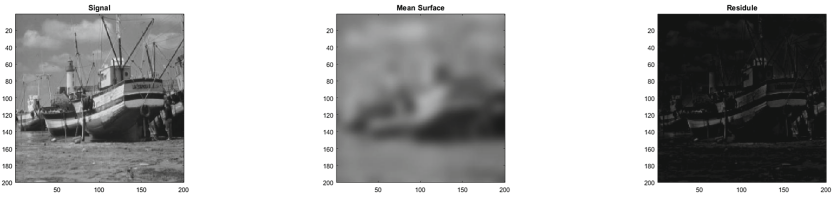

Fig. 4. Left: Original *Boat* image. **Middle:** Mean image $m_a(x, y)$. **Right:** Residual.

to degrees which depend on their frequencies. The results obtained by applying our method to the CSF image are presented in Fig. 3. Once again, the first BIMF contains the highest (horizontal) frequency components of the CSF which appear in the lower right of the image. The next BIMF contains slightly lower (horizontal) frequency components. Our method is seen to perform well in the separation of different (spatially-dependent) frequency components.

Blurred Mean Surface: In Fig. 4 is shown the result of one application of the mean surface extraction method to the 512×512-pixel, 8 bits-per-pixel *Boat* image, using the parameter values $a = 4/\pi^2$ and $T = 50$.

Real Image: In Fig. 5 are shown the results obtained by applying our algorithm to the 256×256-pixel, 8 bpp *Lena* image. Recalling that the sifting process of EMD/BEMD extracts IMFs with successively lower frequencies at each iteration, we note that the major contributions to the first two IMFs produced from the *Lena* image come, as expected, from its edges. Higher-order BIMFs contain lower-frequency features which are centered around the edges.

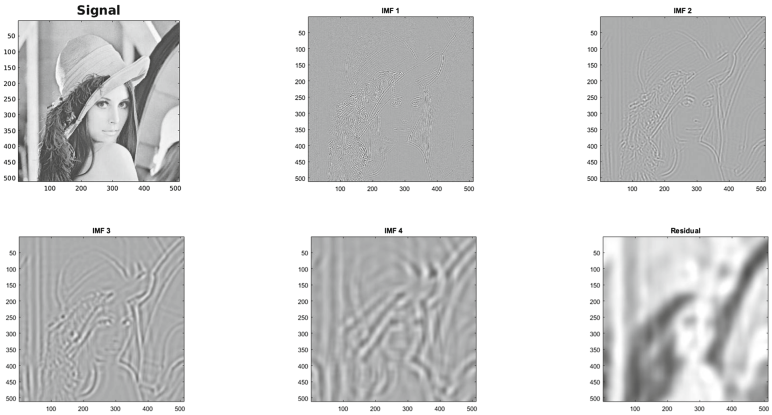

Fig. 5. *Lena* image and its BIMFs. **Top row:** *Lena* image, first and second BIMFs. **Bottom row:** Third and fourth BIMF and the residual.

5.1 Comparison of Computational Costs

Traditional EMD and BEMD methods rely on finding local maxima and minima along with interpolation to find upper and lower envelope. This is computationally expensive, especially in the case of two dimensions, i.e., images. Recall that these procedures are bypassed in our PDE-based approach and replaced by a simple diffusion procedure. As such, our method could potentially require less computational time. To test this conjecture, we have determined the computational times required for a number of iterations of the sifting process for the classical BEMD method as well as our PDE-based BEMD method. (The code based on Flandrin's toolbox [10] was implemented for the classical BEMD method.) The results that obtained by experimenting on the *Lena* image, presented in the first two columns of Table 1, show that our diffusion-based method can decompose a given image into its BIMFs much faster than traditional BEMD.

Table 1. Comparison of computational times for (i) traditional BEMD, (ii) diffusion-based BEMD and (iii) diffusion-based BEMD using Gaussian convolution (GC) in terms of total number of BIMFs computed

	Trad. BEMD	PDE-based EMD	PDE EMD with GC
1. BIMF	4.18 s	1.18 s	0.13 s
2. BIMFs	7.83 s	2.24 s	0.15 s
3. BIMFs	11.16 s	3.38 s	0.27 s
4. BIMFs	13.48 s	4.48 s	0.28 s

An even greater (on the order of tenfold) reduction in computational time is achieved if the finite difference computations involved in the determination of the mean surfaces $m_a(x, y)$ using Eq. (12) are replaced by a single Gaussian convolution, as seen in the final column of Table 1. Technically, the solution of Eqs. (11) or (12) is expressible as Gaussian convolution only in the case that the domain of definition is infinite, i.e., $\mathbb{R}$ or $\mathbb{R}^2$. By using convolution, we are essentially ignoring image boundary effects. In general, the differences between BIMFs obtained by finite differences and convolution are negligible except possibly near the image boundaries.

6 Concluding Remarks

This paper presents a diffusion-based modification of the BEMD algorithm for images. The mean surface of a signal is obtained by evolving the signal with the heat/diffusion equation, therefore avoiding any complicated methods of extracting local maxima and minima and interpolating them. Our approach provides a mathematical interpretation of the EMD algorithm as well as its limitations. The parameters in the diffusion PDE can be adjusted according to the properties

of the signal or image being analyzed. Our algorithm is considerably faster than traditional BEMD. Moreover, it is possible to accelerate the algorithm by using Gaussian convolution. A number of examples have shown that our method can extract multiscale features of images effectively.

Acknowledgements. This research was supported in part by the Natural Sciences and Engineering Research Council of Canada in the form of Discovery Grants (RM and ERV). Financial support from the Faculty of Mathematics and the Department of Applied Mathematics, University of Waterloo (HW) is also gratefully acknowledged.

References

1. Bajaj, V., Pachori, R.B.: Classification of seizure and nonseizure EEG signals using empirical mode decomposition. IEEE Trans. Inf. Technol. Biomed. **16**(6), 1135–1142 (2012)
2. Bhuiyan, S.M., Adhami, R.R., Khan, J.F.: A novel approach of fast and adaptive bidimensional empirical mode decomposition. In: IEEE ICASSP 2008, pp. 1313–1316 (2008)
3. Brodatz, P.: Textures: A Photographic Album for Artists and Designers. Dover, New York (1966)
4. Chen, C.Y., Guo, S.M., Chang, W.S., Tsai, J.S.H., Cheng, K.S.: An improved bidimensional empirical mode decomposition: a mean approach for fast decomposition. Signal Process. **98**, 344–358 (2014)
5. Daubechies, I., Lu, J., Wu, H.T.: Synchrosqueezed wavelet transforms: an empirical mode decomposition-like tool. Appl. Comput. Harm. Anal. **30**(2), 243–261 (2011)
6. Diop, E., Boudraa, A., Khenchaf, A., Thibaud, R., Garlan, T.: Multiscale characterization of bathymetric images by empirical mode decomposition. MARID III, Leeds, UK, pp. 1–3 (2008)
7. El Hadji, S.D., Alexandre, R., Boudraa, A.O.: A PDE model for 2D intrinsic mode functions. In: IEEE ICIP 2009, pp. 3961–3964 (2009)
8. El Hadji, S.D., Alexandre, R., Perrier, V.: A PDE-based and interpolation-free framework for modeling the sifting process in a continuous domain. Adv. Comput. Math. **38**(4), 801–835 (2013)
9. Flandrin, P., Gonçalves, P., Rilling, G.: EMD equivalent filter banks, from interpretation to applications. In: Hilbert-Huang Transform and Its Applications, pp. 99–116. World Scientific (2014)
10. EMD Toolbox. http://perso.ens-lyon.fr/patrick.flandrin/emd.html
11. Gonzalez, R., Woods, R.E., Eddins, S.: Image Database (2010). http://www.imageprocessingplace.com
12. Huang, N.E., Shen, Z., Long, S.R., Wu, M.C., Shih, H.H., Zheng, Q., Yen, N.C., Tung, C.C., Liu, H.H.: The empirical mode decomposition and the Hilbert spectrum for nonlinear and non-stationary time series analysis. Proc. R. Soc. Lond. A **454**, 903–995 (1998)
13. Lei, Y., Lin, J., He, Z., Zuo, M.J.: A review on empirical mode decomposition in fault diagnosis of rotating machinery. Mech. Syst. Signal Process. **35**(1), 108–126 (2013)
14. Liu, G., Li, L., Gong, H., Jin, Q., Li, X., Song, R., Chen, Y., Chen, Y., He, C., Huang, Y.: Multisource remote sensing imagery fusion scheme based on bidimensional empirical mode decomposition (BEMD) and its application to the extraction of bamboo forest. Remote Sens. **9**(1), 19 (2016)

15. Niang, O., Thioune, A., El Gueirea, M.C., Deléchelle, E., Lemoine, J.: Partial differential equation-based approach for empirical mode decomposition: application to image analysis. IEEE Trans. Image Process. **21**(9), 3991–4001 (2012)
16. Nunes, J.C., Bouaoune, Y., Delechelle, E., Niang, O., Bunel, P.: Image analysis by bidimensional empirical mode decomposition. Image Vis. Comput. **21**(12), 1019–1026 (2003)
17. Robson, J.: Spatial and temporal contrast-sensitivity functions of the visual system. J. Opt. Soc. Am. **56**(8), 1141–1142 (1966)
18. Trusiak, M., Patorski, K., Wielgus, M.: Adaptive enhancement of optical fringe patterns by selective reconstruction using FABEMD algorithm and Hilbert spiral transform. Opt. Express **20**(21), 23463–23479 (2012)
19. Wang, H.M., Mann, R., Vrscay, E.R.: A novel forward-PDE approach as an alternative to empirical mode decomposition, preprint (2018)
20. Xu, Y., Liu, B., Liu, J., Riemenschneider, S.: Two-dimensional empirical mode decomposition by finite elements. Proc. R. Soc. Lond. A **462**, 3081–3096 (2006)
21. Yeh, M.H.: The complex bidimensional empirical mode decomposition. Signal Process. **92**(2), 523–541 (2012)